Analytical Methods

PAPER

View Article Online
View Journal | View Issue

Cite this: *Anal. Methods*, 2016, **8**, 418

Green fluorescent protein-based assays for high-throughput functional characterization and ligand-binding studies of biotin protein ligase†

Samuel P. Askin, Thomas E. H. Bond and Patrick M. Schaeffer*

Received 24th November 2015
Accepted 25th November 2015

DOI: 10.1039/c5ay03064a

www.rsc.org/methods

In *E. coli* and other prokaryotes such as *Staphylococcus aureus*, and *Mycobacterium tuberculosis*, biotin protein ligase (BirA) is an emerging drug target as it is the sole enzyme capable of biotin transfer onto the BCCP subunit of ACC. There is currently a gap in simple yet efficient assays for rapidly identifying and characterising inhibitors targeting BirA. We present for the first time the development and validation of a simple and reliable DSF-GTP assay for the high-throughput screening of BirA:ligand interactions using a new GFP-tagged BirA of *E. coli*. In addition, we developed a new GFP-based biotinylation activity assay taking advantage of a GFP tethered with an AviTag. The data obtained with these assays revealed new insights into how the binding of individual or combinations of ligands affect the overall thermal stability and affinity of BirA. The DSF-GTP assay has a Z' value of 0.785 that makes it an excellent tool for future high-throughput screening of inhibitory compounds.

Introduction

Drug discovery is a rapidly expanding and diversifying field. This is in part due to the need to identify alternatives to current therapeutics which are failing as a result of emerging global antibiotic resistance by prevalent bacteria. Strategies to combat antibiotic resistance centre upon the identification of novel compounds to inhibit already established drug targets, identification of new drug targets or target pathways, or a combination of the two. In identifying novel targets in a disease, there is a necessity to comprehensively characterize the target. This allows screening in optimal conditions for monitoring activity or stability of the target as well as a prior, in-depth understanding of specific ligand interactions of the target.

A critical pathway to survival of both eukaryotes and prokaryotes that is targeted in new therapies is fatty acid biosynthesis.[1] In *E. coli*, fatty acid biosynthesis reactions are processed by individual enzymes, following the type II fatty acid synthase pathway. The fatty acid biosynthesis pathway in *E. coli* is well characterized and begins *via* the catalysis of the conversion of acetyl-CoA to malonyl-CoA by the acetyl-coA carboxylase (ACC). Critical to this process is the transfer of biotin to the biotin carboxyl carrier protein (BCCP) subunit of ACC. ACC, and hence the entire fatty acid biosynthesis pathway, is therefore dependent on the synthesis, concentration, and downstream processing of biotin.[2,3]

In *E. coli* and other prokaryotes such as *Staphylococcus aureus*, and *Mycobacterium tuberculosis*, biotin protein ligase (BirA) is an emerging drug target as it is the sole enzyme capable of biotin transfer onto the BCCP subunit of ACC.[4–6] Further to this, the BirA of *E. coli* also regulates expression of bio genes and subsequently biotin synthesis through binding to the biotin operator (*bioO*), a 40 bp inverted repeat that overlaps and controls both biotin operon promoters.[7,8] The apoform of BirA (apoBirA) binds to biotin and ATP which are converted to the adenylated intermediate biotinyl-5′-AMP (bio-5′-AMP) with the release of PPi.[9] The bio-5′-AMP:BirA complex has been described as the holoform of the protein (holoBirA). Biotin is subsequently transferred by holoBirA onto BCCP. The formation of an amide bond between the bio-5′-AMP and a single lysine residue of the BCCP subunit allows for downstream processing of fatty acid chain extension to then take place. The holoBirA also acts as a co-repressor through its binding to *bioO*.[7,10–16]

The interactions between BirA and its ligands have been extensively studied *via* numerous methods. However, the development of high-throughput (HT) assays capable of screening large libraries of inhibitors in a drug screening context has been limited.[17] The emergence of technologies such as differential scanning fluorimetry (DSF), led by the widely adopted Thermofluor assay,[18] has been enterprizing in the field of drug discovery and protein characterization for their ability to profile thousands of conditions simultaneously in small volumes. Recently, a new DSF platform based on the screening of GFP-tagged proteins (DSF-GTP) was developed to profile protein thermal stability in high-throughput (HT).[19–21] This new

Comparative Genomics Centre, James Cook University, DB21, James Cook Drive, Townsville, QLD 4811, Australia. E-mail: patrick.schaeffer@jcu.edu.au; Fax: +61 7 4781 6078; Tel: +61 7 4781 4448

† Electronic supplementary information (ESI) available. See DOI: 10.1039/c5ay03064a

platform does not require the addition of a solvatochromic dye to the reaction thus eliminating the possibility of interferences with protein–ligand interactions. DSF-GTP has also the added advantage that it can be performed in the presence of additional proteins.

Here, we describe for the first time the development and validation of a DSF-GTP assay for the HT screening of BirA:ligand interactions using a new GFP-tagged BirA of *E. coli*. In addition, taking advantage of GFP and the GFP-tagged BirA we developed a suite of new sensitive fluorescence-based secondary screening and activity assays for BirA in preparation for future screening of inhibitory compounds and to decipher their mechanisms of action.

Materials and methods

Cloning, expression and purification of proteins

The GFP-AviTag vector (pSA241) was cloned by digesting the GFP-HA coding vector pIM057 [22] and the AviTag vector pSA236 [23] with KpnI, and dephosphorylation of pSA236 overhangs to prevent vector reclosing. The GFP sequence from pIM057 was then ligated into the digested pSA236 to produce pSA241. The direction of insert ligation was checked by colony PCR following transformation into *E. coli* DH12S cells.

BirA and BirA-GFP expression vectors were derived from pIM022 (pETc-GK-GFP).[19] The BirA coding sequence was amplified from *E. coli* DH12S genomic DNA using the primers psJCU319: 5′-AAAAAACTTAAGAAGGATAACACCGTGCCACTG-3′ and psJCU320: 5′-AAAAAAGCTAGCTTTTTCTGCACTACGCAGGG-3′. The PCR product was digested with NheI and ligated into an EcoRV and NheI digested pIM022 to produce p6HIS-BirA-GFP (pSA239). The plasmid pSA239 was digested with NheI and an end-filling reaction performed to introduce a stop codon between the BirA and GFP coding regions to form p6HIS-BirA (pSA267) using a previously described method.[19]

BirA was expressed and purified as previously described.[23] GFP-AviTag was expressed and purified similarly to a previously described procedure.[24] BirA-GFP was expressed in *E. coli* Single Step KRX competent cells (Promega). *E. coli* Single Step KRX cells were transformed with pSA239 and grown in LB media supplemented with ampicillin (100 μg ml^{-1}) overnight at 37 °C, shaken at 200 rpm. 100 ml cultures of LB supplemented with ampicillin (100 μg ml^{-1}) were then inoculated and incubated at 37 °C with shaking at 200 rpm until the optical density (OD_{600}) reached ~1, at which time expression of BirA-GFP was induced with 0.1% (final) rhamnose. Temperature was then reduced to 16 °C and incubation with shaking continued until OD reached 3–5. Cells were harvested, lysed and purified by Ni-affinity chromatography as previously described,[24] however cell pellets were resuspended in BirA buffer (25 mM Tris (pH 8), 100 mM NaCl, 5% v/v glycerol). BirA-GFP and BirA purity was assessed by SDS-PAGE and quantification performed by Bradford assay.

GFP-based biotinylation activity assay

The biotinylation activity of BirA-GFP was determined analogously to a recently published method.[23] Biotinylation of GFP-AviTag was performed in 50 μl reactions containing 0.3 μM BirA-GFP, 0.5 mM biotin, 2.5 mM ATP, 1 mM $MgCl_2$ and 30 μM GFP-AviTag in 25 mM Tris (pH 8.0). Control reactions without BirA-GFP were performed in parallel. Reactions were incubated at room temperature for 1 h. Following incubation, biotin was removed from the reactions by Ni-affinity purification using Profinity IMAC nickel resin (Biorad) and 1.5 ml spin columns. Reactions were bound to 50 μl pre-equilibrated nickel resin slurry for 5 min at 4 °C, then passed through the resin twice by centrifugation at 1000 × *g* for 1 min at 4 °C. The resin was washed twice with 500 μl of 25 mM Tris (pH 8.0) supplemented with 5% glycerol and 150 mM NaCl by centrifugation at 1000 × *g* for 1 min at 4 °C. The proteins were eluted from the spin columns with 50 μl of the same buffer supplemented with 200 mM imidazole and centrifugation at 1000 × *g* for 1 min at 4 °C following 5 min incubation at 4 °C. The eluate was then passed a second time through the same spin column as for first elution.

Following purification, 7.5 μl of protein elution from spin column (see above) with or without BirA-GFP were incubated with 0.75 μl Stv (streptavidin, 5 mg ml^{-1}, Invitrogen) at room temperature for 15 min in duplicate. Reactions were then subjected to SDS-PAGE and the fluorescence of GFP-AviTag analysed by integration of protein bands (ImageJ, NIH, USA) to determine the extent of biotinylation through binding to Stv. Control reactions were performed similarly by omitting BirA-GFP or Stv as indicated (*cf.* Fig. 1A). An additional control reaction was performed including the addition of competing biotin (0.3 mM) to Stv prior to addition to the reacted GFP-AviTag. All control reactions were processed in identical fashion

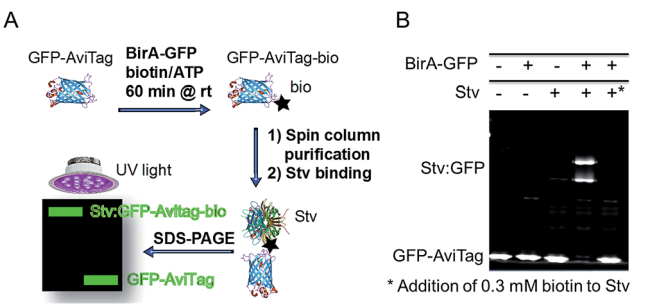

Fig. 1 GFP-based biotinylation activity assay. (A) Schematic representation of the GFP-based biotinylation activity assay workflow. Recombinant GFP-AviTag (30 μM) is reacted at room temperature for 1 h with recombinant BirA-GFP (0.3 μM) in the presence of ATP (2.5 mM), biotin (0.5 mM) and $MgCl_2$ (1 mM) for biotinylation of the AviTag in 25 mM Tris–HCl (pH 8). The biotinylated GFP-AviTag (GFP-AviTag-bio) is then bound to a 1.5 ml spin column containing Ni-affinity resin to eliminate excess biotin. The bound GFP-AviTag-bio is eluted in buffer containing 200 mM imidazole by centrifuging at 1000*g*. Following elution, GFP-AviTag-bio is incubated with excess streptavidin (Stv) for 15 min at room temperature and subjected to SDS-PAGE. Samples are loaded without a heat-denaturation step to allow for direct in-gel fluorescence detection of GFP. Fluorescent proteins are analysed by direct UV-irradiation of the gel and integration of GFP fluorescence. (B) Detection of GFP-AviTag biotinylation by SDS-PAGE and Stv-induced band-shift analysis. Biotinylation reactions were performed and processed as described in Fig. 1A. Control reactions were performed in the absence of BirA-GFP and Stv, or by saturating Stv with excess biotin (*) as indicated.

for comparison to account for protein losses occurred during purification and reaction steps and for normalization. Three independent experiments were performed.

Electrophoretic mobility shift assay

Oligonucleotides psJCU349 5′-TAATCGACTTGTAAACCAAATTGAAAAGATTTAGGTTTACAAGTCTACAC-3′ and psJCU350 5′-GTGTAGACTTGTAAACCTAAATCTTTTCAATTTGGTTTACAAGTCGATTA-3′ (400 μM in 25 mM Tris, 50 mM NaCl) comprising the *bioO* 40 bp sequence with 5 bp flanking sequences (underlined) were mixed together and annealed by heating at 80 °C for 2 min followed by slow cooling to room temperature (rt).

All reactions contained 1 μM BirA-GFP, 1 μM *bioO*, 10 mM Tris (pH 8), 0.83% glycerol and 50 mM NaCl. In addition to these components some reactions were spiked with 0.83 mM biotin, 0.83 mM ATP and $MgCl_2$, and combinations thereof as indicated in Fig. 2A. All reactions were incubated at rt for 15 min, then analysed by agarose gel electrophoresis followed by staining with GelRed and integration of fluorescent bands (ImageJ, NIH, USA).

Size exclusion chromatography

For SEC analysis of apo- and holoBirA-GFP, BirA-GFP (100 μl at 20 μM in BirA buffer) was combined with 100 μl of either : 25 mM Tris (pH 8) or 25 mM Tris (pH 8) supplemented with 2 mM of biotin, ATP and $MgCl_2$. For SEC in the presence of *bioO*, BirA-GFP was first mixed with *bioO* (100 μl at 20 μM each in BirA buffer) and incubated for 10 min at rt prior to mixing with 100 μl of 25 mM Tris (pH 8) supplemented with 2 mM of biotin, ATP and $MgCl_2$. All reactions were incubated for 10 min at rt. The reactions were then injected in a Superdex 200 10/300 GL column (GE Lifesciences) equilibrated in BirA buffer using a Biologic Duoflow Chromatography System (Biorad) with a flowrate of 0.25 ml min^{-1}. Following fractionation of BirA-GFP, 200 μl of each fraction was analysed using a fluorescence plate reader (Victor 3V Wallac 1420, Perkin-Elmer) set to 355 nm excitation/535 nm emission.

SEC analysis of BirA was performed as described above, however the concentrations of BirA and *bioO* were increased 10-fold in all cases. UV absorbance was used to determine the peaks and quaternary structure of BirA in each of the conditions. Fractions containing the peak expected to be the *bioO*:BirA dimer (10 μl) were also analysed by SDS-PAGE followed by Coomassie Blue staining (*cf.* ESI Fig. S2†).

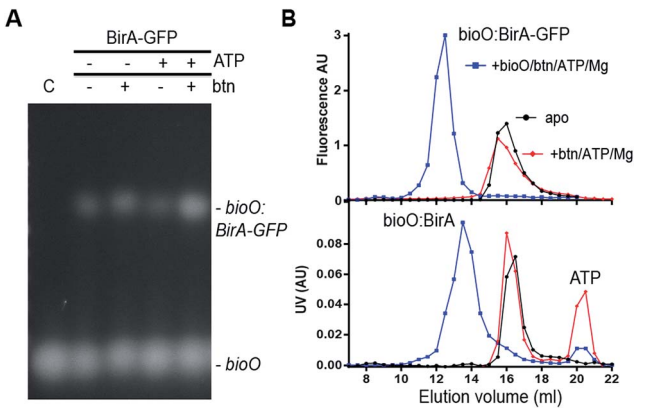

Fig. 2 DNA-binding activity and dimerization of BirA-GFP and BirA. (A) Determination of *bioO*-binding to BirA-GFP by EMSA. BirA-GFP (1 μM) was reacted with *bioO* (0.5 μM) in the presence of 1 mM biotin, 1 mM ATP or 1 mM biotin, 1 mM ATP and 1 mM $MgCl_2$ for 10 min at rt. Reactions were then analysed by agarose gel electrophoresis and GelRed staining. The positions of free *bioO* probe (C) and shifted bands are indicated. Identical experiments were also performed with BirA (*cf.* ESI Fig. S1†). (B) Top: SEC analysis of BirA-GFP. BirA-GFP (10 μM) was injected either alone, in the presence of 1 mM biotin, 1 mM ATP and 1 mM $MgCl_2$, or in the presence of *bioO* (10 μM), 1 mM biotin, 1 mM ATP and 1 mM $MgCl_2$. The proteins were detected through the fluorescence of the GFP domain of BirA-GFP. Bottom: SEC analysis of BirA. Reactions were as described for BirA-GFP, however BirA and *bioO* were present at 100 μM each and protein peaks were determined by UV absorption.

DSF-GTP assay

All reactions (50 μl) containing 3 μM BirA-GFP were performed in a reaction buffer consisting of 15 mM Tris–HCl (pH 8), 10 mM NaCl and 0.5% (v/v) glycerol. Ligands and additives were added to the reaction buffer as indicated in the following sections. All reactions were equilibrated for 10 min at rt prior being subjected to melt-curve analysis using a real-time thermal cycler (IQ5 iCycler, Bio-Rad). Temperature range was set from 35–85 °C, increasing in 0.5 °C increments every 30 s. Data was analysed as previously described.[20] All reactions were performed at least in duplicates.

Biotin and ATP dependence. To determine the effect of biotin on the T_m of BirA-GFP, reactions were performed with increasing concentrations of biotin ranging from 500 nM to 1 mM as indicated in Fig. 3. To determine the combined effects of ATP and biotin, reactions were performed with increasing concentrations of both species ranging from 500 nM to 1 mM and 1 mM $MgCl_2$. To determine the effect of ATP on the T_m of biotin-bound BirA-GFP, reactions were performed with increasing concentrations of ATP ranging from 500 nM to 1 mM, 1 mM biotin and 1 mM $MgCl_2$.

Nucleotide specificity. To determine the effect of different nucleotides on the T_m of BirA-GFP, reactions were performed in the presence of 1 mM of either ATP, CTP, UTP or GTP and 1 mM $MgCl_2$. To determine the effect of different nucleotides on the T_m of biotin-bound BirA-GFP, reactions were performed as above in the presence of 1 mM biotin. All nucleotide stocks were buffered (pH 8).

Results and Discussion

Biotin transfer activity of BirA and BirA-GFP

The production of a functional GFP-tagged BirA (BirA-GFP) was required for the DSF-GTP assay. First, the biotinylation activity of BirA-GFP was determined with a new GFP-based biotinylation activity assay to assess whether GFP-tagging of BirA was not detrimental to its activity. The new assay relies on complex formation between a biotinylated GFP containing the AviTag biotinylation sequence (GLNDIFEAQKIEWHE)[25–28] and

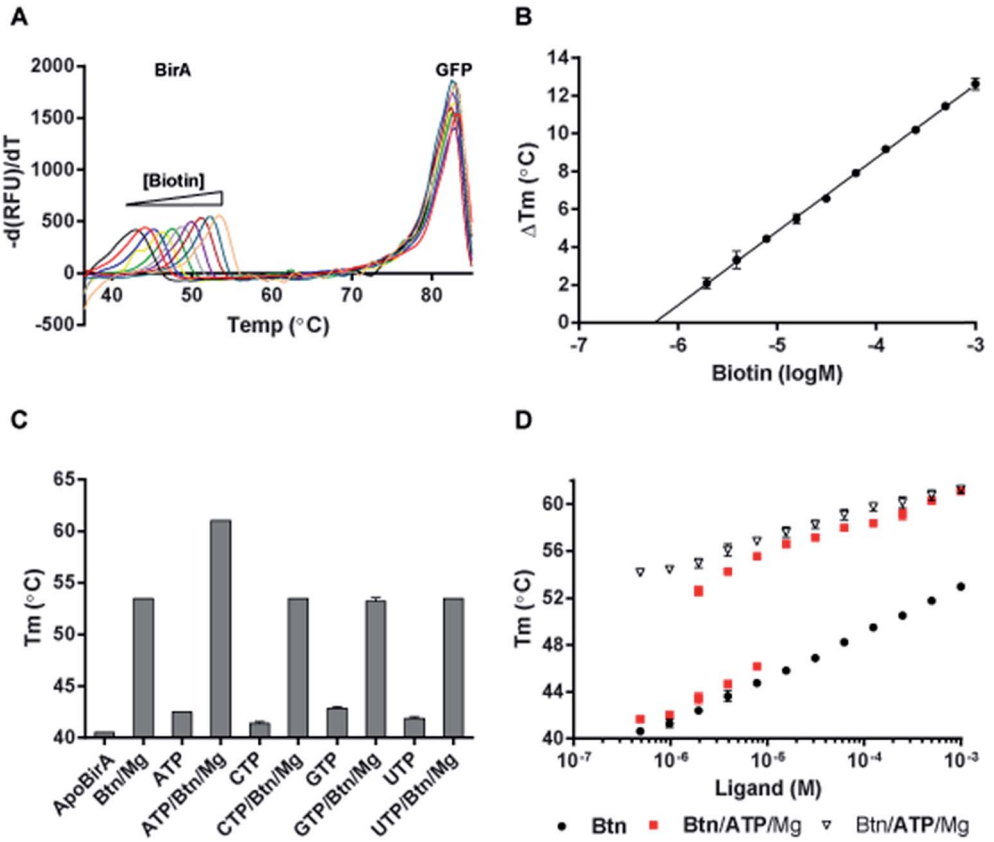

Fig. 3 Thermal stability of BirA-GFP by DSF-GTP. (A) DSF-GTP melt-curves (−d(RFU)/dT) demonstrating the effect of increasing biotin concentrations on BirA-GFP thermal stability. BirA-GFP (3 μM) was reacted with increasing concentrations of biotin ranging from 500 nM to 1 mM for 10 min at rt prior to analysis by DSF-GTP. (B) The concentration dependence of biotin on T_m of BirA-GFP. ΔT_m values were calculated by subtracting T_m of apoBirA-GFP from the T_m obtained in presence of increasing [biotin]. (C) Nucleotide specificity of BirA-GFP. Effect of different nucleotides (1 mM) as indicated on the T_m of BirA-GFP in the presence or absence of 1 mM biotin and $MgCl_2$. BirA-GFP was reacted with each nucleotide (with or without biotin/$MgCl_2$). (D) Comparison of the effect of simultaneous increase of [biotin], [ATP] and [$MgCl_2$] (red squares) *vs.* independent increase of [ATP] in the presence of 1 mM biotin and $MgCl_2$ (open triangles) on BirA-GFP T_m. Reactions of BirA-GFP with increasing [biotin] (black circles) were also performed for comparison. For all experiments, error bars represent standard deviations ($n = 3$).

a streptavidin (Stv) probe[23] resulting in an electrophoretic mobility shift of the complex detectable by SDS-PAGE (Fig. 1A). The GFP-based biotinylation activity assay is identical in principle to our recent 'in-gel biotin–protein conjugate detection assay'.[23] Here, a new AviTag-labelled GFP (GFP-AviTag) was developed and used as substrate for BirA-GFP. GFP-AviTag (30 μM) was biotinylated by BirA-GFP at room temperature (rt) for 1 h. After removal of excess biotin the biotinylated GFP-AviTag was bound to Stv and analysed by SDS-PAGE. For this assay it is important to not heat-denature the samples before loading onto the polyacrylamide gel to avoid loss of the GFP fluorophore. The biotinylation activity assay is not intended for measuring enzyme kinetics but it is a useful rapid end-point assay and has the potential to be applied for the identification of biotinylation inhibitors.

In-gel fluorescence quantitation of the reacted GFP-AviTag showed that BirA-GFP was able to biotinylate ~96% of the protein in 1 h at rt (Fig. 1B). Abolition of biotinylated GFP-AviTag:Stv complex formation by the addition of 0.3 mM biotin to Stv prior addition of GFP-AviTag (Fig. 1B, far right lane) confirmed that the GFP-shift observed was the result of Stv binding. Faint higher order bands were visible in those wells that Stv was included. These were due to a protease contamination present in the commercial Stv sample (data not shown). However the level of proteolysis was negligible in the context of determining the activity of BirA-GFP and did not affect quantitation. The level of biotinylation obtained with BirA-GFP and the GFP-AviTag corresponds well to *in vitro* biotinylation activity levels previously reported by us and others for a variety of tagged and untagged BirA.[23,29] Indeed, BirA and BirA-GFP yielded almost identical levels of biotinylated AviTag probes in the same conditions[23] demonstrating that the tagging of BirA does not significantly affect its activity.

Dimerization and DNA-binding activity of BirA and BirA-GFP

A 50 bp double strand oligonucleotide consisting of the 40 bp *bioO* sequence flanked at either end by 5 bp of natural chromosomal sequences was used to test the DNA-binding activities of BirA (*cf.* ESI Fig. S1†) and BirA-GFP (Fig. 2A). The binding of BirA and BirA-GFP to *bioO* was analysed by EMSA demonstrating that the presence of the GFP did not significantly affect

BirA DNA-binding activity. Previous studies have shown that holoBirA binds with the greatest affinity to *bioO* – *i.e.* in the presence of the co-repressor bio-5′-AMP.[7,30,31] The biotin-bound BirA and apoBirA bind cooperatively to *bioO* with ~10-fold and ~50-fold lower affinity respectively than holoBirA,[31] and this was also evident with our GFP-tagged species in our high-salt conditions (Fig. 2A). The same difference in affinity was also confirmed with the BirA species (*cf.* ESI Fig. S1†).

The quaternary structure of BirA and BirA-GFP was then analysed by size exclusion chromatography (SEC). BirA (injected at 100 μM initial concentration) was detected by UV absorption whereas BirA-GFP could be analysed by fluorimetry at a ten-fold lower concentration (*i.e.* 10 μM initial concentration). Both proteins remained in a monomeric form in their apoforms. Previous data have shown that apoBirA and the biotin-bound form can dimerize in low salt conditions at mM concentrations.[31] These complexes would therefore not be observed in our high-salt SEC conditions. A slight shift was observed for both holoBirA and holoBirA-GFP (Fig. 2B). These shifts in elution suggest a dramatic change in conformation of the proteins or a fast exchanging dimer form in our SEC conditions. Previous studies indicate that dimerization of holoBirA is influenced by ionic strength with reported K_D values for dimerization of ~1 and 10 μM in low- and high-salt respectively.[30,31] As expected, a dramatic shift in elution was observed for both holoBirA and holoBirA-GFP upon addition of *bioO* reflecting their dimer formation and *bioO* binding (Fig. 2B and C; ESI Fig. S2†). The high sensitivity of the fluorimetric SEC assay compared to UV detection, makes it an attractive secondary assay for the identification of molecules capable of interfering with dimer formation and DNA-binding activity of BirA-GFP.

HT characterization of BirA-GFP by DSF-GTP

The structural and functional characterization of BirA-GFP in the previous sections demonstrated that the tethering of GFP has no effect on BirA activity. The use of DSF-GTP requires that a transition in the melting curve can be observed corresponding to the BirA domain unfolding before complete loss of GFP fluorescence at ~80 °C (Fig. 3A). We identified a clear transition in the melting curve of BirA-GFP and validated the assay with increasing concentrations of biotin for which increasing transition midpoint (T_m) values could be recorded as illustrated in Fig. 3A. For this, BirA-GFP (3 μM) was reacted with increasing concentrations of biotin ranging from 488 nM–1 mM for 10 min at rt, prior to determination of T_m by DSF-GTP. Fig. 3B illustrates the perfect correlation between BirA-GFP thermal stability and biotin concentration obtained from data presented in Fig. 3A. The thermal stability of BirA-GFP (~41 °C) increased progressively by up to ~12.5 °C in the presence of 1 mM biotin (Fig. 3A and B). A best-fit trendline was obtained with a *R*-square value > 0.99 reflecting the excellent reproducibility of the assay. The quality of the new HT DSF-GTP assay for BirA was further assessed by *Z*′-factor[32] determination which yielded an excellent Z' value of 0.785 ($n = 96$).

BirA-GFP was then profiled for nucleotide specificity both alone and in combination with biotin and $MgCl_2$. When the effect of nucleotides alone was investigated, the T_m of BirA-GFP increased only by ~2 °C with 1 mM ATP. GTP was the most stabilizing ~2.9 °C, and CTP and UTP the least stabilizing <2 °C. Interestingly, the T_m of BirA-GFP was increased by ~12 °C in the presence of 1 mM biotin, and by ~20.5 °C when reacted with both 1 mM biotin and ATP (*i.e.* leading to formation of bio-5′-AMP; Fig. 3C). We did not observe any cumulative stabilizing effects for UTP, CTP or GTP that could suggest the formation of higher affinity intermediates with these species in the presence of biotin. The large increase in T_m of BirA-GFP upon binding of both ATP and biotin suggesting the formation of bio-5′-AMP is well supported by the recently reported K_D of 50 pM for the holocomplex.[33] Our data correlates well with the sequential binding of biotin and ATP by BirA, with biotin binding first leading to the formation of a specific ATP binding site.[13–15,34–36] This site is largely non-existent and nonspecific prior to biotin binding. A disordered loop of the apoBirA structure (*i.e.* residues 212–233) known as the adenylate binding loop (ABL) is involved in ATP binding.[36] The ABL becomes ordered upon binding of ATP by BirA and folds over it.[15]

BirA has previously been shown to have very low *in vitro* biotinylation activity with CTP (~10%) and GTP (~5%).[17] Our data suggests that GTP binds marginally better to the non-specific binding pocket of apoBirA-GFP in the absence of biotin. Nevertheless, considering the very low affinity of BirA for all nucleotides in the absence of biotin (Fig. 3C) and the total absence of cumulative stabilisation with GTP, CTP and UTP in the presence of biotin, it is unlikely that any of these nucleotides could lead to formation of the ABL in the absence of biotin. The low biotinylation activity of BirA observed in the presence of high concentrations of CTP or GTP[17] could therefore only be explained by reaction of BirA-bound biotin with GTP or CTP without ABL formation. To our knowledge, this is the first study of the sequential binding of different nucleotides and their specificity to the ATP binding site using DSF.

We have previously been able to estimate the apparent binding parameters (K_{obs}) of glycerol kinase and Tus for their respective ligands with DSF-GTP in conditions of [ligand] > [protein] using a simple graphical method. In both cases, the K_{obs} were in agreement with the dissociation constants (K_D) obtained with alternative quantitative methods.[20,21] K_{obs} is defined as the concentration of ligand at which the titration curve trendline for a given ligand (Fig. 3D) intercepts with log[ligand]-axis at the T_m of the unliganded protein. The thermal slopes are identical within a protein for different ligands since they are determined by the unfolding enthalpy.[37] It is therefore important to note that K_{obs} is not directly comparable to K_D although changes in K_{obs} will be proportional to changes in K_D. Using our simple graphical method we obtained a K_{obs} of 231 nM (ESI Table S1†) which was ~5-fold higher than the previously reported K_D of 45 nM[38] – similar to the range of endogenous biotin concentration in *E. coli.* The difference observed between our K_{obs} and the previously reported K_D may potentially be due to the different conditions and pH in our study as well as temperature effects and possible steric hindrances from the GFP.

Next, we investigated the combined effect of ATP and biotin leading to bio-5′-AMP production on BirA-GFP's thermal stability (Fig. 3D). Based on the K_D of 50 pM that has recently been reported for the holoBirA complex, we expected that a sharp increase in BirA-GFP thermal stability would occur upon bio-5′-AMP production resulting in a sigmoidal titration curve around ligand concentrations corresponding to the BirA-GFP concentration used in the reaction as well as the presence of two peaks corresponding to the unbound and bound protein form. For this, two different experimental setups were performed: (a) the effects of serial dilutions of an equimolar solution of ATP and biotin were analysed on BirA-GFP T_m; and (b) the concentration of biotin was kept constant and the effects of serial dilutions of ATP were analysed. When [biotin] was kept constant (1 mM) and [ATP] was varied, the lowest concentration of ATP tested (500 nM) was not stabilizing BirA-GFP beyond the effect of 1 mM biotin (*cf.* Fig. 3D; black circles). A very small sigmoidicity was observed at ~2 μM ATP followed by a steady increase in BirA-GFP T_m with higher ATP concentrations (Fig. 3D). When both [biotin] and [ATP] were increased simultaneously (Fig. 3D; red squares), two distinct BirA-GFP T_m peaks were observed between 1.9–7.8 μM immediately suggesting a K_D < 10 nM as expected. One T_m peak corresponded to the effect of biotin only (Fig. 3D; black circles) and the other T_m peak that was sharply increased – *i.e.* converging towards the curve obtained for fixed [biotin] with increasing [ATP] (Fig. 3D; open triangles) – most likely corresponded to the holoBirA-GFP complex. When the concentration of ligands was >8 μM, only the higher T_m peaks were observed reflecting the curve obtained for fixed [biotin] with increasing [ATP] (Fig. 3D; *cf.* open triangles with red squares). As the increase in BirA-GFP T_m is very sharp >1 μM biotin and ATP – *i.e.* much more than would be expected for merely additive effects of biotin and ATP – we can conclude that the very sharp increase in BirA-GFP T_m reflects formation of the tighter bio-5′-AMP:BirA-GFP complex. It also suggests that binding of biotin significantly increases the affinity for ATP by several orders of magnitude through formation of the biotin-induced ATP binding site and ABL.

The titration curve obtained with biotin (Fig. 3D; black circles) has a much steeper slope than the ones obtained in the presence of both ATP and biotin (Fig. 3D; open triangles and red squares) revealing that the biotin-bound BirA-GFP form might have a significantly smaller enthalpy of unfolding compared to the ATP and biotin form. This argument has to be taken with caution due to the complexity of the system. Indeed, formation and dissociation of the bio-5′-AMP adduct which binds much tighter than biotin and ATP to BirA-GFP, might be limiting steps influencing the slope of these titration curves. Nevertheless, due to the linearity of the titration curves suggesting 100% conversion of ATP and biotin into bio-5′-AMP (Fig. 3D and ESI Table S1†) we decided to determine the K_{obs} values from the two different experimental setups. Here, a K_{obs} of 3.3 pM was obtained in increasing [biotin] and [ATP] which was similar to the K_{obs} of 7.4 pM in constant [biotin] and increasing [ATP]. These K_{obs} values reflected quite well the tight affinity and K_D of BirA with the bio-5′-AMP adduct (*i.e.* 50 pM in 200 mM KCl and pH 8) reported by Eginton *et al.*[33] although our reactions were performed with the natural substrates ATP and biotin, in low salt and slightly higher pH conditions.

To our knowledge this is the first time that the biotin-induced conformational changes leading to ATP binding and bio-5′-AMP:BirA-GFP complex could be analysed by DSF in such depth. Overall the combined analyses of nucleotide specificity and ligand concentration dependence demonstrate the versatility and breadth of information that can be easily and rapidly gained using DSF-GTP for BirA-GFP characterization.

Conclusions

In this study, we demonstrate the utility and high quality of a new HT DSF-GTP assay for the high-throughput characterization of BirA ($Z' = 0.785$), an emerging drug target for antibiotic development. BirA could be fused to a C-terminal GFP without the requirement for any further solubility tags for high-level production of soluble and functional proteins. BirA-GFP was fully functional when compared to BirA and was able to biotinylate ~96% of GFP-AviTag in 1 h at rt. Our results obtained with the different natural BirA ligands reflected well the previously known properties of BirA as well as revealed new insights into how its binding to individual or combinations of ligands affects the overall thermal stability of the protein. With the validation of *E. coli* BirA-GFP in the new DSF-GTP, SEC, EMSA and GFP-based biotinylation activity assays now at hand, the subject of future work will be to apply this suite of assays for HT screening and identification of BirA inhibitors and to decipher their mechanisms of action and structure activity relationships. It is expected that our workflow will be adaptable to other bacterial BirA orthologs as well as the human holocarboxylase synthetase and that it will significantly streamline their target characterization to screening processes by reducing time and cost.

Conflict of interest

The authors declare that they have no conflict of interest.

References

1 J. W. Campbell and J. E. Cronan, *Annu. Rev. Microbiol.*, 2001, **55**, 305–332.
2 J. W. Campbell and J. E. Cronan, *J. Bacteriol.*, 2001, **183**, 5982–5990.
3 K. Magnuson, S. Jackowski, C. O. Rock and J. E. Cronan, *Microbiol. Rev.*, 1993, **57**, 522–542.
4 N. R. Pendini, M. Y. Yap, S. W. Polyak, N. P. Cowieson, A. Abell, G. W. Booker, J. C. Wallace, J. A. Wilce and M. C. Wilce, *Protein Sci.*, 2013, **22**, 762–773.
5 B. P. Duckworth, K. M. Nelson and C. C. Aldrich, *Curr. Top. Med. Chem.*, 2012, **12**, 766–796.
6 T. P. Soares da Costa, W. Tieu, M. Y. Yap, N. R. Pendini, S. W. Polyak, D. Sejer Pedersen, R. Morona, J. D. Turnidge, J. C. Wallace, M. C. Wilce, G. W. Booker and A. D. Abell, *J. Biol. Chem.*, 2012, **287**, 17823–17832.

7 E. D. Streaker and D. Beckett, *J. Mol. Biol.*, 2003, **325**, 937–948.
8 J. Abbott and D. Beckett, *Biochemistry*, 1993, **32**, 9649–9656.
9 O. Prakash and M. A. Eisenberg, *Proc. Natl. Acad. Sci. U. S. A.*, 1979, **76**, 5592–5595.
10 P. R. Adikaram and D. Beckett, *J. Mol. Biol.*, 2012, **419**, 223–233.
11 E. D. Streaker and D. Beckett, *Protein Sci.*, 2006, **15**, 1928–1935.
12 E. D. Streaker and D. Beckett, *Biochemistry*, 2006, **45**, 6417–6425.
13 L. H. Weaver, K. Kwon, D. Beckett and B. W. Matthews, *Protein Sci.*, 2001, **10**, 2618–2622.
14 L. H. Weaver, K. Kwon, D. Beckett and B. W. Matthews, *Proc. Natl. Acad. Sci. U. S. A.*, 2001, **98**, 6045–6050.
15 Z. A. Wood, L. H. Weaver, P. H. Brown, D. Beckett and B. W. Matthews, *J. Mol. Biol.*, 2006, **357**, 509–523.
16 H. Zhao and D. Beckett, *J. Mol. Biol.*, 2008, **380**, 223–236.
17 B. Ng, S. W. Polyak, D. Bird, L. Bailey, J. C. Wallace and G. W. Booker, *Anal. Biochem.*, 2008, **376**, 131–136.
18 M. W. Pantoliano, E. C. Petrella, J. D. Kwasnoski, V. S. Lobanov, J. Myslik, E. Graf, T. Carver, E. Asel, B. A. Springer, P. Lane and F. R. Salemme, *J. Biomol. Screening*, 2001, **6**, 429–440.
19 M. J. Moreau, I. Morin and P. M. Schaeffer, *Mol. BioSyst.*, 2010, **6**, 1285–1292.
20 M. J. J. Moreau, I. Morin, S. P. Askin, A. Cooper, N. J. Moreland, S. G. Vasudevan and P. M. Schaeffer, *RSC Adv.*, 2012, **2**, 11892–11900.
21 M. J. Moreau and P. M. Schaeffer, *Mol. BioSyst.*, 2013, **9**, 3146–3154.
22 I. Morin, S. P. Askin and P. M. Schaeffer, *Analyst*, 2011, **136**, 4815–4821.
23 A. E. Sorenson, S. P. Askin and P. M. Schaeffer, *Anal.Methods*, 2015, **7**, 2087–2092.
24 D. B. Dahdah, I. Morin, M. J. Moreau, N. E. Dixon and P. M. Schaeffer, *Chem. Commun.*, 2009, 3050–3052, DOI: 10.1039/b900905a.
25 P. J. Schatz, *Bio-Technol.*, 1993, **11**, 1138–1143.
26 D. Beckett, E. Kovaleva and P. J. Schatz, *Protein Sci.*, 1999, **8**, 921–929.
27 M. G. Cull and P. J. Schatz, *Methods Enzymol.*, 2000, **326**, 430–440.
28 M. Howarth and A. Y. Ting, *Nat. Protoc.*, 2008, **3**, 534–545.
29 Y. Li and R. Sousa, *Protein Expression Purif.*, 2012, **82**, 162–167.
30 E. Eisenstein and D. Beckett, *Biochemistry*, 1999, **38**, 13077–13084.
31 E. D. Streaker, A. Gupta and D. Beckett, *Biochemistry*, 2002, **41**, 14263–14271.
32 J. H. Zhang, T. D. Y. Chung and K. R. Oldenburg, *J. Biomol. Screening*, 1999, **4**, 67–73.
33 C. Eginton, W. J. Cressman, S. Bachas, H. Wade and D. Beckett, *J. Mol. Biol.*, 2015, **427**, 1695–1704.
34 K. Kwon, E. D. Streaker, S. Ruparelia and D. Beckett, *J. Mol. Biol.*, 2000, **304**, 821–833.
35 K. Kwon and D. Beckett, *Protein Sci.*, 2000, **9**, 1530–1539.
36 S. Naganathan and D. Beckett, *J. Mol. Biol.*, 2007, **373**, 96–111.
37 D. Matulis, J. K. Kranz, F. R. Salemme and M. J. Todd, *Biochemistry*, 2005, **44**, 5258–5266.
38 K. Kwon, E. D. Streaker and D. Beckett, *Protein Sci.*, 2002, **11**, 558–570.